Role of Drp1 in cigarette smoke extract-induced C2C12 myoblast senescence and mitochondrial dysfunction

Biman Ma,[1] Dan Yang,[2] Huilian Liu,[1] Huibin Lin,[1] Yaoguang Huang,[1] Lanchun Sun[1]

[1]Department of Pulmonary and Critical Care Medicine, Zhanjiang Central Hospital, Zhanjiang, Guangdong
[2]Department of Pulmonary and Critical Care Medicine, Guangdong State Farms Central Hospital, Zhanjiang, Guangdong, China

ABSTRACT

Sarcopenia is a frequent comorbidity of chronic obstructive pulmonary disease (COPD), which is strongly associated with prolonged cigarette smoke exposure. This study investigated the effects of cigarette smoke extract (CSE) on an immortalized murine C2C12 myoblast model, focusing on apoptosis, proliferation, cellular senescence, and mitochondrial function. C2C12 myoblasts were exposed to graded concentrations of CSE (0.75%, 1.5%, and 3%). Cell viability and proliferation were assessed by Cell Counting Kit-8 (CCK-8) and ethynyl-2'-deoxyuridine (EdU) assays, respectively. Apoptosis was quantified by flow cytometry, and cellular senescence was evaluated by SA-β-galactosidase staining. Mitochondrial membrane potential (ΔΨm) was assessed by tetramethylrhodamine ethyl ester (TMRE) staining, and mitochondrial fluorescence was evaluated using MitoTracker staining. Drp1 protein expression was determined by Western blotting, while Drp1, Fis1, Mff, and Mitofusin 1/2 mRNA levels were analyzed by RT-qPCR. To assess the contribution of Drp1 expression, a rescue experiment was performed using Drp1 overexpression. CSE exposure reduced C2C12 cell viability and proliferation, increased apoptosis and SA-β-Gal-positive cells, lowered ΔΨm, and reduced MitoTracker-positive fluorescence. Drp1 protein expression and Drp1, Fis1, and Mff mRNA levels decreased, whereas Mitofusin 1/2 mRNA levels increased. Drp1 overexpression attenuated CSE-associated senescence and mitochondrial dysfunction. These findings indicate that altered Drp1 expression is associated with CSE-induced myoblast senescence and mitochondrial homeostatic disruption *in vitro*.

Key words: chronic obstructive pulmonary disease with sarcopenia; cigarette smoke extract; dynamin-related protein 1; cellular senescence; mitochondrial dysfunction.

Correspondence: Lanchun Sun, MD, Department of Pulmonary and Critical Care Medicine, Zhanjiang Central Hospital, No. 236, Yuanzhu Road, Chikan District, Zhanjiang City 524000, Guangdong, China. E-mail: linhui19700830@163.com

Contributions: Biman Ma, investigation, formal analysis, validation, visualization, writing – original draft. Dan Yang, methodology, software, writing – review & editing. Huilian Liu, investigation, data curation. Huibin Lin, investigation, validation. Yaoguang Huang, investigation. Lanchun Sun, conceptualization, supervision, funding acquisition, project administration, writing – review & editing.

Funding: this study was supported by the Medical Scientific Research Foundation of Guangdong Province (Grant No. B2026620).

Conflict of interest: the authors declare no competing interests, and all authors confirm accuracy.

Data Availability Statement: all data supporting the results of this study are available from the corresponding author upon reasonable request.

Introduction

Cigarette smoking constitutes the primary etiology of chronic obstructive pulmonary disease (COPD), which is ranked as the third-most prevalent cause of death worldwide currently.[1] COPD is clinically defined by persistent airflow obstruction and respiratory manifestations,[2] frequently presenting with multisystem comorbidities that span cardiovascular, gastrointestinal, hematological, musculoskeletal, and additional physiological systems.[3] Sarcopenia, a cardinal extrapulmonary manifestation featuring diminished age-related muscle strength, mass, and physical function,[4] demonstrates an epidemiological prevalence of 27.5% in COPD populations. Stratified by disease severity, its occurrence escalates significantly from 19.1% in GOLD I-II to 37.6% in GOLD III-IV patients, establishing a direct proportionality between sarcopenia burden and COPD progression.[5] Cigarette smoke (CS) thus constitutes a primary driver of skeletal muscle aging, with elucidation of its underlying pathophysiology offering pivotal insights for developing new therapies.

Mounting evidence positions mitochondrial impairment as a core driver of pulmonary pathology, where persistent defective mitochondria actively fuel COPD development.[6,7] Mitochondria operate as cellular sentinels by integrating metabolic flux with nuclear signaling. This unique positioning confers dual capacity for environmental threat sensing and injury adaptation, executed through ROS emission, membrane polarity shifts, and MAM-protein signaling pathways.[8] The counterbalancing processes of mitochondrial fission and fusion constitute a critical regulatory axis, maintaining structural integrity, bioenergetic competence, and adaptive resilience under physiological stress. As the primary executor of mitochondrial fission, dynamin-related protein 1 (Drp1) operates predominantly within the cytosol. Upon activation, it assembles higher-order oligomers with mitochondrial outer membrane receptors to scaffold division machinery, including Fis1, Mff, MiD49, and MiD51. The fission process is precisely orchestrated through post-translational modifications (PTMs) that modulate Drp1's GTPase activity.[9,10]

Muscle wasting in sarcopenia arises through synergistic mechanisms, declining mitochondrial bioenergetics, impaired satellite cell activation, disrupted anabolic-catabolic equilibrium, and persistent pro-inflammatory cascades.[11,12] Emerging evidence positions mitochondrial dysregulation as the central orchestrator of sarcopenia pathogenesis, where fission/fusion dynamics, biogenesis, and mitophagy collectively sustain skeletal muscle proteostasis.[13] This investigation examined dose-dependent effects of cigarette smoke extract (CSE) on C2C12 myoblast proliferation, apoptosis, and senescence, delineating mechanisms underlying mitochondrial fission-fusion rebalancing. Subsequent analyses assessed whether preserving mitochondrial homeostasis attenuates CSE-induced cellular senescence, proposing novel geroprotective strategies against CS-driven skeletal muscle aging.

Materials and Methods

Preparation of CSE

Cigarette smoke extract was generated by passing mainstream smoke of five cigarettes (tar: 10 mg/cig; nicotine: 0.9 mg/cig; CO: 12 mg/cig) through 10 mL serum-free high-glucose DMEM (Dulbecco's Modified Eagle Medium, 11965-118; Gibco, Rockville, MD, USA), pre-warmed to 37°C. Cigarettes were machine-smoked for 5 minutes under constant airflow. The resulting extract was adjusted to pH 7.4 and sterile-filtered through a 0.22 μm membrane. To standardize preparations between batches, we spectrophotometrically quantified the extract at 320 nm; solutions achieving a mean optical density (OD) of 4.0 were designated as 100% CSE (with inter-batch variations maintained below 5%). Freshly prepared CSE was utilized within 30 min of generation.

Cell culture and CSE treatment

C2C12 murine myoblasts (Immocell, Xiamen, China) were cultured in high-glucose DMEM containing 10% fetal bovine serum (FBS, FSD500; ExCell Bio, Taicang, China) and 100× penicillin-streptomycin (C0222; Beyotime, Shanghai, China), at 37°C/5% CO_2 with 95% humidity. For subculture at >80% confluency, cells were treated with 1 mL 0.25% trypsin-EDTA (R001100; Gibco) for 1 min at 37°C. Trypsinization was terminated by adding 2 volumes of complete medium upon visible cell rounding and detachment. Cells were then reseeded for subculture. For the dose-response experiments, CSE exposure was 24 h for the CCK-8, flow cytometry, TMRE, MitoTracker, Western blot, and RT-qPCR assays, and 48 h for the SA-β-Gal and EdU assays. In the rescue experiments, cells were transfected for 48 h as described below and then exposed to 3% CSE for the assay-specific duration stated above.

Transfection

For cellular transfection, the Drp1 overexpression plasmid (OE-Drp1) and the corresponding empty vector pcDNA3.1-NC were constructed by GenChem (Shanghai, China). Following the manufacturer's protocol, transfection of cells with either Drp1 overexpression plasmid or negative control vector was performed for 48 h in serum-free medium using Lipofectamine 3000 (Invitrogen, Waltham, MA, USA).

CCK-8 assays

Cells were plated at 2,000 cells/well in 96-well plates and allowed to adhere for 6 h under standard conditions (37°C, 5% CO_2). Cells were then exposed to the designated CSE concentrations for 24 h. Six wells were used as technical replicates within each independent experiment. Ten microliters of CCK-8 solution (BA00208; Bioss, Beijing, China) was added to each well 2 h before assay termination. Absorbance at 450 nm was recorded using a Multiskan FC microplate reader (357-714018; Thermo-Fisher Scientific, Waltham, MA, USA).

Cell apoptosis was detected by flow cytometry

Log-phase cells were seeded in 6-well plates at 1×10□ cells/well. After 12-h serum starvation post-adhesion, cells were exposed to the designated CSE concentrations for 24 h at 37°C and 5% CO_2. Cells were then resuspended in fresh medium, transferred to centrifuge tubes, and pelleted at 1,000 rpm for 5 min (Cence, HT200R, Changsha, China). Supernatants were aspirated prior to apoptosis analysis using an Annexin V-FITC kit (C1062L; Beyotime) according to the manufacturer's protocol. Samples were acquired within 1 hour on an Attune NxT flow cytometer (Thermo-Fisher Scientific).

SA-β-Gal staining kit

Cells grown in 6-well plates to approximately 50-60% confluence were exposed to the designated CSE concentrations for 48 h. Following one wash with PBS, cellular senescence was assessed using the SA-β-Gal Staining Kit (Beyotime) according to the manufacturer's protocol, with cells stained while still attached. Senescent cells were visualized and quantified under a light microscope.

OPEN ACCESS

MitoTracker fluorescence staining

Cells (1×10^6/well) were seeded in 6-well plates. Following 12-h serum starvation after adhesion, cells were exposed to the designated CSE concentrations for 24 h. Mitochondria were labeled with MitoTracker Green, and nuclei were counterstained with DAPI. Fluorescence images were acquired under identical microscope settings for all groups. The MitoTracker-positive fluorescence area was quantified for each biological replicate and normalized to the control group.

TMRE staining

Logarithmic-phase cells were plated in 6-well plates at 1×10^6 cells/well. Cells were exposed to the designated CSE concentrations for 24 h at 37°C and 5% CO_2. Culture medium was aspirated and cells rinsed once with PBS. Cells were incubated with 1 mL TMRE working solution (pre-warmed to 37°C) for 30 min under standard culture conditions. Post-incubation, supernatant was removed and cells washed twice with pre-warmed complete medium. After adding 2 mL fresh pre-warmed medium, mitochondrial membrane potential was assessed via fluorescence microscopy using 549 nm excitation / 575 nm emission filters.

Western blot

Cells in log-phase growth were seeded into six-well plates at a density of 1×10^6 cells per well and cultured for 24 hat 37°C in a humidified atmosphere containing 5% CO_2. After the indicated transfection where applicable, cells were exposed to the designated CSE concentration for 24 h. Following removal of the culture medium, adherent cells underwent two washes with ice-cold phosphate-buffered saline (PBS). Total cellular proteins were subsequently extracted from each well using 0.5 ml of RIPA lysis buffer (P0013; Beyotime), supplemented with phenylmethylsulfonyl fluoride (PMSF). Protein concentrations were quantified using a bicinchoninic acid (BCA) assay kit (WB6501; NCM Biotech, Suzhou, China). Equal amounts of protein lysate were combined with 5× SDS-PAGE loading buffer (WB2001; NCM Biotech) and denatured by boiling. Denatured protein samples were resolved *via* electrophoresis on 10% Tris-glycine sodium dodecyl sulfate-polyacrylamide gel electrophoresis (SDS-PAGE) gels. Separated proteins were then electrophoretically transferred onto polyvinylidene difluoride (PVDF) membranes. Non-specific binding sites on the membranes were blocked through a 1-h incubation at room temperature with 5% (w/v) non-fat dry milk dissolved in Tris-buffered saline with Tween 20 (TBST). The blocked membranes were probed overnight at 4°C with the following primary antibodies: anti-Drp1 rabbit monoclonal antibody (#8570, dilution 1:1000; Cell Signaling Technology, Danvers, MA, USA) and anti-GAPDH mouse monoclonal antibody (ab8245, dilution 1:10000; Abcam, Cambridge, MA, USA). After three washes with PBS containing 0.1% Tween 20 (PBST) to remove unbound primary antibody, membranes were incubated with appropriate horseradish peroxidase (HRP)-conjugated secondary antibodies for 1 hour at 37°C. Following three additional PBST washes, immunoreactive protein bands were detected using an enhanced chemiluminescence (ECL) substrate kit (P2100, NCM Biotech) according to the manufacturer's instructions.

RT-qPCR

Cells at logarithmic growth phase were seeded into six-well plates at an initial density of 1×10^6 cells per well and cultured under standard conditions (37°C, 5% CO_2, humidified atmosphere) for 24 h. Upon reaching 80-90% confluency, cells underwent serum starvation for 12 h prior to the designated treatment. After the indicated transfection where applicable, cells were exposed to the designated CSE concentration for 24 h. After supernatant removal, 500 µL of lysis buffer (RC112; Vazyme, Nanjing, China) was added directly to each well for cell digestion and lysis. cDNA was synthesized from total RNA using the HiScript III 1st Strand cDNA Synthesis Kit (R312; Vazyme). qPCR was performed on a CFX96 Touch™ system (1855195; Bio-Rad, Hercules, CA, USA) with Taq Pro Universal SYBR qPCR Master Mix (Q712; Vazyme). Gene expression was analyzed *via* the 2-ΔΔCt method. The thermocycling protocol is detailed in Table 1. The primer sequences are shown in Table 2.

Table 1. qPCR cycling parameters.

Stage	Reaction	Cycles	Temperature	Time
1	Initial denaturation	1	95°C	30 sec
2	Amplification	40	95°C	10 sec
			60°C	10 sec
3	Dissociation curve	1	95°C	15 sec
			65°C	60 sec
			95°C	15 sec

Table 2. The primer sequences.

Primers	Sequence (5'→3')	
Drp1	F	GCCTCAGATCGTCGTAGTGG
	R	ACCCCATTCTTCTGCTTCAACT
Fis1	F	CAGTGTTGCGTGTTAAGGGATGAA
	R	TTCAAAATTCCTTGCAGCTTCGT
Mff	F	TCACATTTGGTGAGTGGGGC
	R	TTTTCCGGGACCCTCATTCG
Mitofusin 1/2	F	GACAAAGCCAGAGTCCTTCAGA
	R	TGTGACTCCAGCTTATCTCTTGG
GAPDH	F	GGAGAGTGTTTCCTCGTCCC
	R	ATGAAGGGGTCGTTGATGGC

Statistical analysis

Statistical analyses and graphical representations were conducted using GraphPad Prism software (Version 9.4.0, GraphPad Inc., La Jolla, CA, USA). Unless otherwise stated, all experiments were independently repeated three times (three biological replicates); technical replicates, where used, were averaged within each biological replicate before statistical analysis. Continuous variables are expressed as mean ±SD. Intergroup comparisons were assessed through unpaired two-tailed Student's *t*-tests or one-way analysis of variance (ANOVA), with Tukey's *post-hoc* test applied where appropriate. Statistical significance threshold was established at $p<0.05$ for all analyses.

Results

CSE induces cellular senescence in C2C12 cells

To investigate the effect of CSE on senescence-related phenotypes in mouse C2C12 myoblasts, cells were treated with 0.75%, 1.5%, and 3% CSE for the assay-specific durations described in the Methods. Cell viability, assessed using the CCK-8 assay after 24 h exposure, showed a dose-dependent reduction compared with the control group (Figure 1A). Flow cytometry after 24 h exposure demonstrated that all three CSE concentrations increased apoptosis in C2C12 cells, with higher concentrations yielding increased apoptotic rates (Figure 1 B,C). SA-β-Gal staining after 48 h exposure showed increased β-Gal activity following CSE treatment (Figure 1D). EdU staining after 48 h exposure revealed a dose-dependent suppression of cellular proliferation in CSE-treated cells (Figure 1 E,F).

CSE induces mitochondrial dysfunction and morphological abnormalities in C2C12 cells

Prompted by the observed effects of CSE on C2C12 cell proliferation, apoptosis, and senescence phenotypes, we further examined mitochondrial changes. Mitochondrial membrane potential (ΔΨm) was assessed using TMRE staining after 24 h CSE exposure. TMRE, a cell-permeant, mitochondria-specific red fluorescent dye, rapidly accumulates in mitochondria driven by the negative membrane potential, with higher fluorescence intensity correlating with greater ΔΨm. Compared with the control, CSE treatment dose-dependently reduced ΔΨm in C2C12 cells (Figure 2 A,B), indicating mitochondrial dysfunction. MitoTracker staining performed after 24 h CSE exposure showed a dose-dependent reduction in the relative MitoTracker-positive fluorescence area (Figure 2 C,D).

CSE inhibits Drp1 expression

Expression levels of mitochondrial fission/fusion proteins in C2C12 myoblasts were quantified using Western blot analysis and RT-qPCR, respectively. Compared to the control group, CSE significantly reduced Drp1 protein expression ($p<0.05$) in a dose-dependent manner (Figure 3A-B). RT-qPCR analysis further revealed that CSE treatment markedly decreased mRNA levels of the fission proteins Drp1, Fis1, and Mff, whereas mRNA levels of the fusion proteins mitofusin 1/2 were increased (Figure 3C).

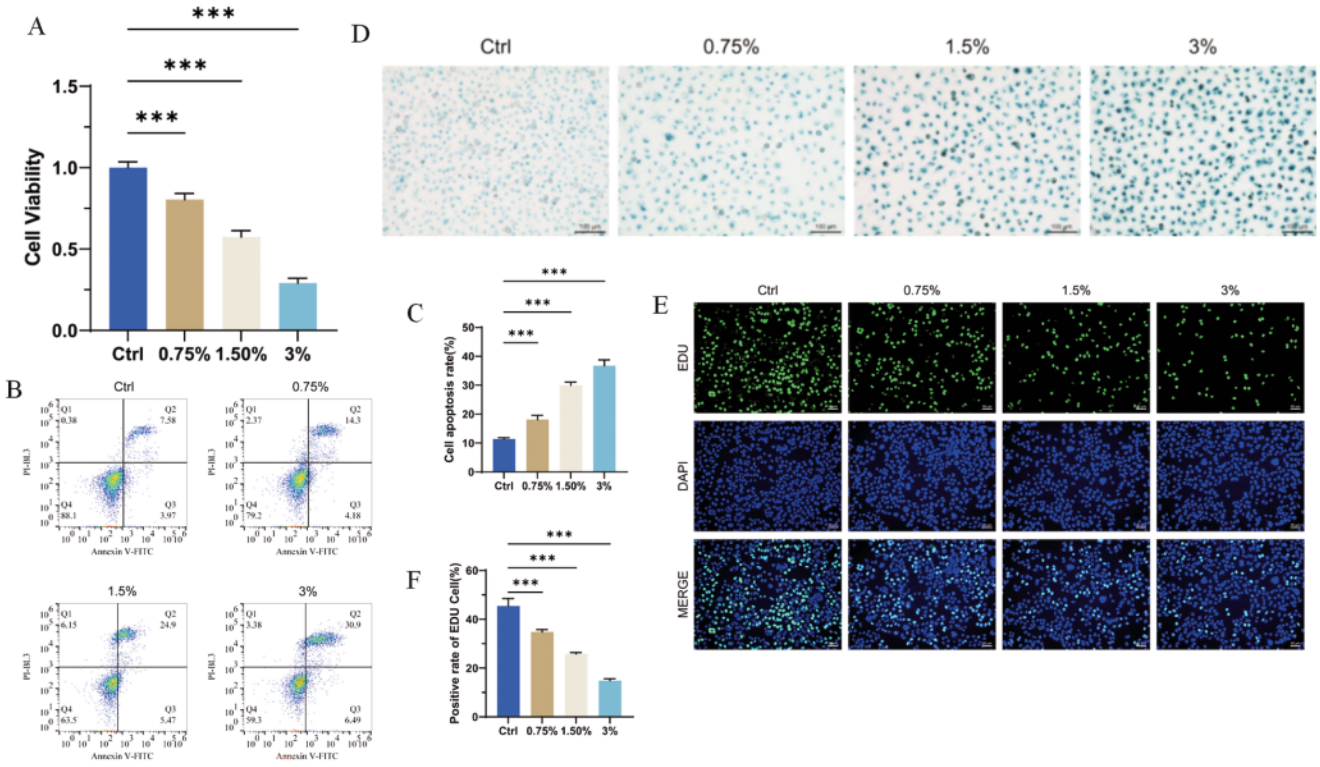


Figure 1. CSE treatment inhibits C2C12 cell proliferation and promotes senescence and apoptosis. **A**) Cell viability assessed by CCK-8 assay following treatment with graded concentrations of CSE. **B,C**) Apoptosis levels quantified by flow cytometry. **D**) Cellular senescence visualized by SA-β-galactosidase (SA-β-Gal) staining. **E,F**) Edu staining for detection of cell proliferation.

OPEN ACCESS

Overexpression of Drp1 rescues C2C12 cells from CSE-induced senescence

Drp1 was overexpressed in C2C12 cells via plasmid transfection. SA-β-Gal staining revealed increased cellular senescence following 3% CSE treatment compared to the control group, whereas Drp1 overexpression attenuated this senescence phenotype relative to the 3% CSE-treated group (Figure 4A); 3% CSE treatment induced mitochondrial dysfunction in C2C12 cells, an effect rescued by Drp1 overexpression (Figure 4 B,C). Western blot analysis demonstrated reduced Drp1 protein expression after 3% CSE exposure; conversely, Drp1 overexpression substantially elevated Drp1 protein levels (Figure 4 D,E). Similarly, 3% CSE treatment decreased mRNA levels of Drp1, Fis1, and Mff while increasing Mitofusin 1/2 mRNA, alterations that were reversed by Drp1 overexpression (Figure 4F).

Discussion

Sarcopenia involves a reduction in both muscle fiber number and size, with molecular pathways implicating cellular senescence.[14] Key features of senescence -telomere attrition, genomic instability, epigenetic shifts, proteostatic failure, mitochondrial dysfunction, and impaired nutrient sensing- are detectable in individuals with COPD.[15] CS exposure represents a well-documented risk factor for COPD, where consequent oxidative stress serves as a key driver of cellular senescence mechanisms and their associated secretory phenotype (SASP).[16] CS exposure promotes the expression of senescence markers in epithelial cells and fibroblasts, contributing to pulmonary emphysema pathogenesis, including p16, p19, and p21.[17] Our findings demonstrate that CSE treatment increased the senescent burden, suppressed proliferation, and elevated apoptosis in C2C12 myoblasts. As the molecular pathways through which cigarette smoke promotes C2C12 cellular senescence remain poorly defined, we subsequently focused on delineating these mechanisms.

Mitochondrial dynamics encompass biosynthesis, fusion, and fission processes.[18] Homeostasis between fusion and fission events is essential for sustaining mitochondrial functionality. Key mediators of membrane fusion include mitofusins (Mfn) and optic atrophy 1 (Opa1), which coordinate integration of mitochondrial outer and inner membranes with endosomal compartments.[19] Conversely, fission is primarily governed by Drp1, requiring recruitment of mitochondrial kinetic effectors - including Mff, Fis1, and proteins MID49/MID51 (also termed mitochondrial dynamics proteins 51 and 49).[20,21] Dysregulation of mitochondrial dynamics accompanies cellular aging, yet the functional contribution of fusion/fission machinery to the aging process remains contentious. Accumulating evidence reveals impaired mitochondrial fission in senescent cells, with studies demonstrating that enhancing fission-related protein expression (notably Drp1) improves cellular physiology. Aged rats exhibit reduced Drp1 levels in aortic endothelium compared to young counterparts, a decline coinciding with autophagosome accumulation. This Drp1 downregulation is implicated in initiating mitochondrial dysfunction, elevated mitochondrial ROS production, impaired autophagic flux, and ultimately, endothelial cell senescence and dysfunction.[22] Genetic or pharmacological inhibition of PUM2 activity augments Mff mRNA translational efficiency, potentially restoring homeostatic mechanisms during aging.[23] Contradictory evidence indicates senescence drives mitochondrial fission bias, precipitating metabolic perturbations. Treatment with Yiqihuoxue decoction (GSC) restored mitochondrial morphology in endothelial progenitor cells (EPCs), concurrently attenuating Drp1, Mff, and Fis1 protein expression, reducing mtROS and ATP levels, and improving mitochondrial function, collectively ameliorating D-gal-induced cellular senescence.[24] Klf5 downregulation reduces eIF5a expression,

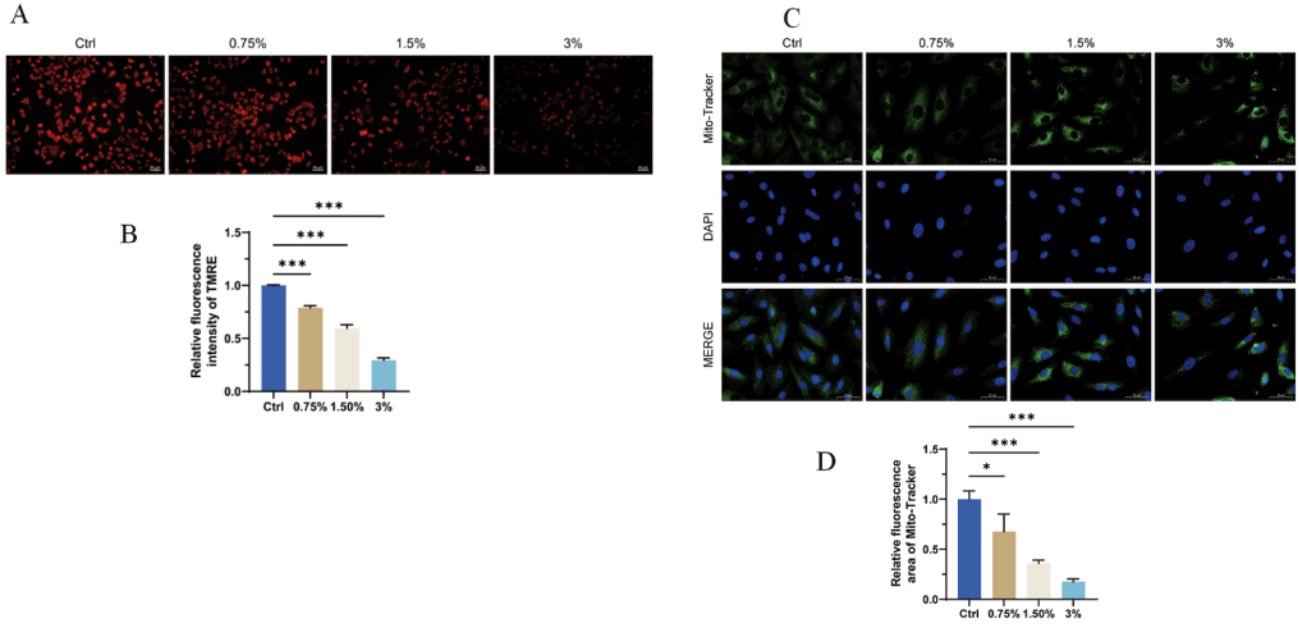


Figure 2. CSE treatment induces mitochondrial dysfunction in C2C12 cells after 24 h exposure. **A,B**) Alterations in mitochondrial membrane potential (ΔΨm) detected by TMRE staining. **C**) MitoTracker Green fluorescence (green) with DAPI nuclear counterstaining (blue). **D**) Quantification of the relative MitoTracker-positive fluorescence area.

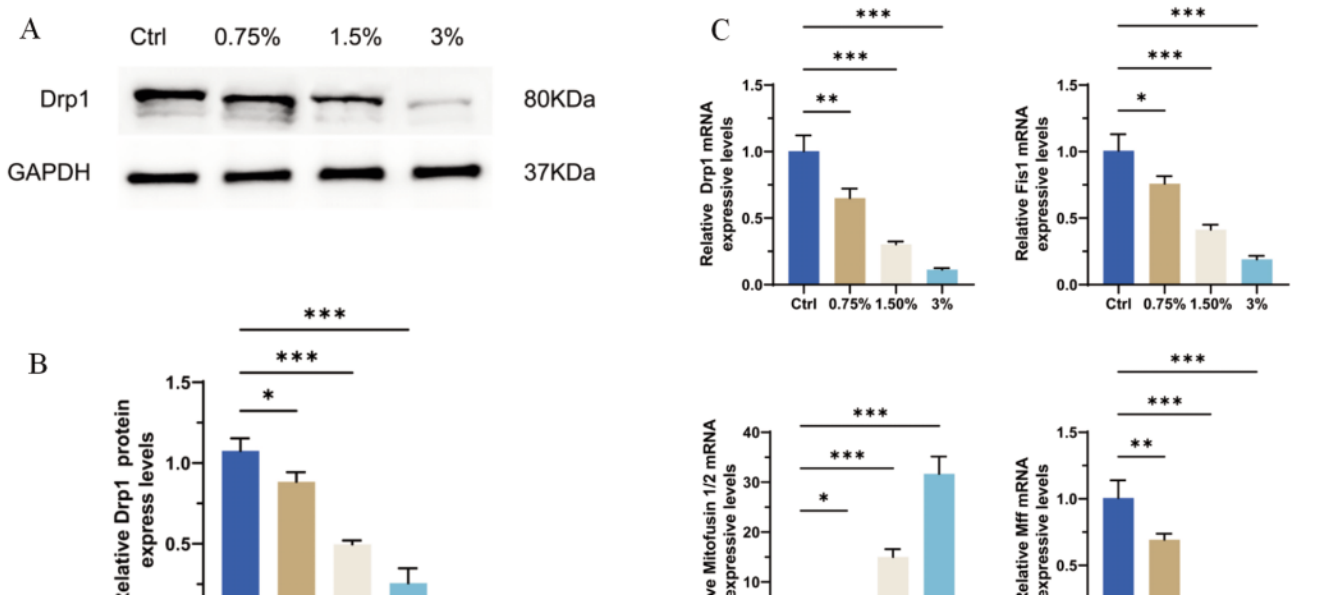


Figure 3. CSE treatment modulates the expression levels of mitochondria-associated proteins in C2C12 cells. **A,B**) Drp1 protein expression levels in C2C12 cells detected and quantified by Western blot analysis following CSE treatment. **C**) Drp1, Fis1, Mff, and Mitofusin 1/2 mRNA expression levels in C2C12 cells detected by RT-qPCR following CSE treatment.

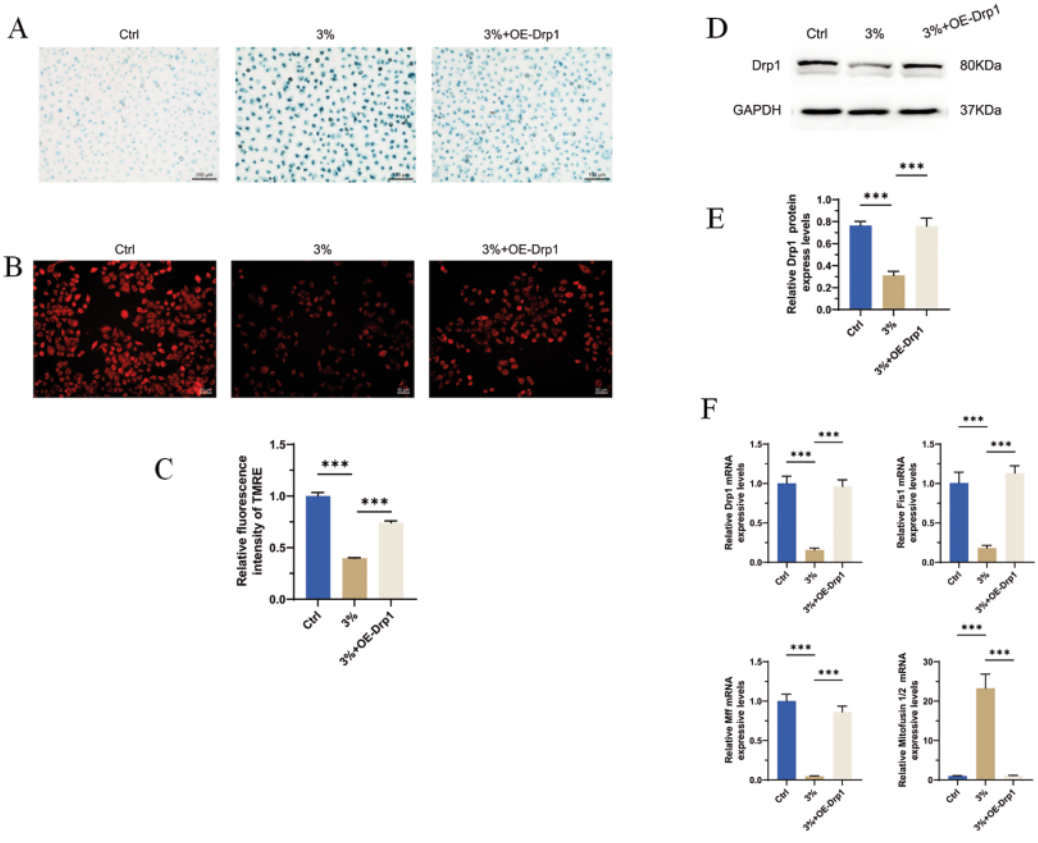


Figure 4. Overexpression of Drp1 ameliorates CSE-induced senescence in C2C12 cells by maintaining mitochondrial homeostasis. **A**) Detection of cellular senescence levels by SA-β-Gal staining. **B,C**) Alterations in mitochondrial membrane potential (ΔΨm) detected by TMRE staining. **D,E**) Drp1 protein expression levels in C2C12 cells detected and quantified by Western blot analysis. **F**) mRNA expression levels of Drp1, Fis1, Mff, and Mitofusin 1/2 in CSE-treated cells detected by RT-qPCR.

OPEN ACCESS

driving excessive mitochondrial fission and ROS overproduction. Suppressing mitochondrial fission curtails ROS generation and attenuates VSMC senescence.[25] Our data demonstrate that cigarette smoke extract suppresses Drp1 expression in murine C2C12 myoblasts, exacerbating mitochondrial compromise. This finding appears contradictory to currently reported mechanisms. Substantial evidence implicates Drp1 in promoting pathological mitochondrial fission during CSE-induced cellular damage. For instance, human bronchial epithelial (HBE) cells exposed to CSE demonstrate significantly reduced MFN2 and OPA1 expression alongside elevated Drp1 levels. Crucially, Drp1 suppression mitigates inflammatory responses in this model.[26] Pulmonary specimens from COPD patients exhibit impaired mitochondrial fusion, pathologically augmented mitophagy, and concomitant cellular senescence. Upregulation of MFN2 and OPA1 counteracts oxidative stress, normalizes mitophagic flux, and attenuates lung cell senescence.[27] Notably, experimental evidence supports our findings: Genetic ablation of Drp1 or Fis1 induces mitochondrial tubule elongation, whereas ectopic expression of either protein reverts these elongated networks to basal morphology.[28] Recent work demonstrates that Drp1 ablation forestalls mitochondrial conversion from tubular networks to fragmented ultrastructures, concomitantly extending chronological lifespan in fungal models.[29] Paradoxically, abrogated mitochondrial fission promotes organellar oxidative lesions that precipitate neuronal demise in mammalian systems.[30]

Several limitations in this study require acknowledgment. First, the findings are solely derived from cellular-level experiments using the C2C12 myoblast model, limiting direct extrapolation to *in vivo* physiological or pathological contexts. Second, while we demonstrate that Drp1 overexpression rescues CSE-induced senescence and mitochondrial dysfunction, the precise molecular mechanism underlying Drp1's functional role remains incompletely resolved. Drp1 activity is critically regulated by post-translational modifications (PTMs), such as phosphorylation (e.g., at Ser616 or Ser637) and SUMOylation, which can dramatically alter its subcellular localization, GTPase activity, and oligomerization state independently of total protein abundance. Our focus on transcriptional and total protein expression levels does not capture these essential regulatory layers. Consequently, the observed discrepancies between our results (showing reduced total Drp1 protein/mRNA) and reports linking cigarette smoke to enhanced Drp1 activity and mitochondrial fragmentation may stem from unmeasured PTM-driven activation. Future investigations directly assessing Drp1 PTM status (e.g., activation-linked phosphorylation) in this model would provide deeper mechanistic insights and potentially reconcile these divergent observations. Accordingly, the present data support an association between Drp1 expression and the observed CSE-induced phenotype but do not establish total Drp1 abundance as the sole determinant of the underlying mechanism. In this *in vitro* C2C12 model of CSE-induced myoblast injury and senescence, CSE exposure suppressed cellular proliferation while promoting senescence and apoptosis. Drp1 overexpression attenuated these changes and improved indices of mitochondrial homeostasis. These findings support a role for altered Drp1 expression in CSE-associated myoblast dysfunction, while further studies are required to define the underlying regulatory mechanism.

References

1. Singh D, Agusti A, Anzueto A, Barnes PJ, Bourbeau J, Celli BR, et al. Global strategy for the diagnosis, management, and prevention of chronic obstructive lung disease: the GOLD science committee report 2019. Eur Respir J 2019;53:1900164.
2. Rabe KF, Watz H. Chronic obstructive pulmonary disease. Lancet 2017;389:1931-40.
3. Vanfleteren LEGW, Spruit MA, Wouters EFM, Franssen FME. Management of chronic obstructive pulmonary disease beyond the lungs. Lancet Respir Med 2016;4:911-24.
4. O'Dell A, Diegel-Vacek L, Burt L, Corbridge S. CE: Managing Stable COPD: An Evidence-Based Approach. Am J Nurs 2018;118:36-47.
5. Sepúlveda-Loyola W, Osadnik C, Phu S, Morita AA, Duque G, Probst VS. Diagnosis, prevalence, and clinical impact of sarcopenia in COPD: a systematic review and meta-analysis. J Cachexia Sarcopenia Muscle 2020;11:1164-76.
6. Larson-Casey JL, He C, Carter AB. Mitochondrial quality control in pulmonary fibrosis. Redox Biol 2020;33:101426.
7. Schumacker PT, Gillespie MN, Nakahira K, Choi AMK, Crouser ED, Piantadosi CA, et al. Mitochondria in lung biology and pathology: more than just a powerhouse. Am J Physiol Lung Cell Mol Physiol 2014;306:L962-74.
8. Naviaux RK. Metabolic features of the cell danger response. Mitochondrion 2014;16:7-17.
9. Losón OC, Song Z, Chen H, Chan DC. Fis1, Mff, MiD49, and MiD51 mediate Drp1 recruitment in mitochondrial fission. Mol Biol Cell 2013;24:659-67.
10. Atkins K, Dasgupta A, Chen KH, Mewburn J, Archer SL. The role of Drp1 adaptor proteins MiD49 and MiD51 in mitochondrial fission: implications for human disease. Clin Sci (Lond) 2016;130:1861-74.
11. Cruz-Jentoft AJ, Sayer AA. Sarcopenia. Lancet 2019;393: 2636-46.
12. Basse AL, Agerholm M, Farup J, Dalbram E, Nielsen J, Ørtenblad N, et al. Nampt controls skeletal muscle development by maintaining Ca(2+) homeostasis and mitochondrial integrity. Mol Metab 2021;53:101271.
13. Yan X, Shen Z, Yu D, Zhao C, Zou H, Ma B, et al. Nrf2 contributes to the benefits of exercise interventions on age-related skeletal muscle disorder via regulating Drp1 stability and mitochondrial fission. Free Radical Bio Med 2022;178:59-75.
14. Aversa Z, Zhang X, Fielding RA, Lanza I, LeBrasseur NK. The clinical impact and biological mechanisms of skeletal muscle aging. Bone 2019;127:26-36.
15. MacNee W. Is chronic obstructive pulmonary disease an accelerated aging disease? Ann Am Thorac Soc 2016;13 Suppl 5:S429-37.
16. Hikichi M, Mizumura K, Maruoka S, Gon Y. Pathogenesis of chronic obstructive pulmonary disease (COPD) induced by cigarette smoke. J Thorac Dis 2019;11:S2129-40.
17. Tuder RM, Kern JA, Miller YE. Senescence in chronic obstructive pulmonary disease. Proc Am Thorac Soc 2012;9:62-3.
18. Chan DC. Mitochondrial dynamics and its involvement in disease. Annu Rev Pathol 2020;15:235-59.
19. Gao S, Hu J. Mitochondrial fusion: the machineries in and out. Trends Cell Biol 2021;31:62-74.
20. Kalia R, Wang RYR, Yusuf A, Thomas PV, Agard DA, Shaw JM, et al. Structural basis of mitochondrial receptor binding and constriction by DRP1. Nature 2018;558:401-5.
21. Forte M, Schirone L, Ameri P, Basso C, Catalucci D, Modica J, et al. The role of mitochondrial dynamics in cardiovascular diseases. Brit J Pharmacol 2021;178:2060-76.
22. Lin JR, Shen WL, Yan C, Gao PJ. Downregulation of dynamin-related protein 1 contributes to impaired autophagic

flux and angiogenic function in senescent endothelial cells. Arterioscler Thromb Vasc Biol 2015;35:1413-22.
23. D'Amico D, Mottis A, Potenza F, Sorrentino V, Li H, Romani M, et al. The RNA-binding protein PUM2 impairs mitochondrial dynamics and mitophagy during aging. Mol Cell 2019;73:775-87.
24. Liu Y, Niu Z, Wang X, Xiu C, Hu Y, Wang J, et al. Yiqihuoxue decoction (GSC) inhibits mitochondrial fission through the AMPK pathway to ameliorate EPCs senescence and optimize vascular aging transplantation regimens. Chin Med 2024;19:143.
25. Ma D, Zheng B, Liu HL, Zhao YB, Liu X, Zhang XH, et al. Klf5 down-regulation induces vascular senescence through eIF5a depletion and mitochondrial fission. Plos Biol 2020;18:e3000808.
26. Wang Y, Li YJ, Li CC, Pu L, Geng WL, Gao F, et al. GRP78 mediates mitochondrial fusion and fission in cigarette smoke-induced inflammatory responses in airway epithelial cells. Inhal Toxicol 2024;36:511-20.
27. Li C, Liu Q, Chang Q, Xie M, Weng J, Wang X, et al. Role of mitochondrial fusion proteins MFN2 and OPA1 on lung cellular senescence in chronic obstructive pulmonary disease. Resp Res 2023;24:319.
28. Seo AY, Joseph AMRA, Dutta D, Hwang JCY, Aris JP, Leeuwenburgh C. New insights into the role of mitochondria in aging: mitochondrial dynamics and more. J Cell Sci 2010;123:2533-42.
29. Scheckhuber CQ, Erjavec N, Tinazli A, Hamann A, Nyström T, Osiewacz HD. Reducing mitochondrial fission results in increased life span and fitness of two fungal ageing models. Nat Cell Biol 2007;9:99-105.
30. Zhang Z, Kageyama Y, Sesaki H. Mitochondrial division prevents neurodegeneration. Autophagy 2012;8:1531-3.

Received: 12 August 2026. Accepted: 23 September 2026.

This work is licensed under a Creative Commons Attribution-NonCommercial 4.0 International License (CC BY-NC 4.0).
©Copyright: the Author(s), 2026
Licensee PAGEPress, Italy
European Journal of Histochemistry 2026; 70:4753
doi:10.4081/ejh.2026.4753

Publisher's note: all claims expressed in this article are solely those of the authors and do not necessarily represent those of their affiliated organizations, or those of the publisher, the editors and the reviewers. Any product that may be evaluated in this article or claim that may be made by its manufacturer is not guaranteed or endorsed by the publisher.

OPEN ACCESS